College of Engineering Poster Presentations

2013 Undergraduate Research and Scholarship Conference

4-15-2013

# Use of Global Electrochemical Techniques to Characterize Localized Corrosion Behavior on Aluminum Alloys

Joe Croteau
*Department of Materials Science and Engineering, Boise State University*

Kerry N. Allahar
*Department of Materials Science and Engineering, Boise State University*

Darryl P. Butt
*Department of Materials Science and Engineering, Boise State University*

Michael F. Hurley
*Department of Materials Science and Engineering, Boise State University*

# Use of Global Electrochemical Techniques to Characterize Localized Corrosion Behaviors on Aluminum Alloys

Joseph R. Croteau[1] – joecroteau@u.boisestate.edu
Kerry N. Allahar[1,2], Darryl P. Butt[1,2], Michael F. Hurley[1,2]
[1]Boise State University – Department of Materials Science and Engineering
[2]Center for Advanced Energy Studies

BOISE STATE UNIVERSITY
COLLEGE OF ENGINEERING
*Department of Materials Science & Engineering*

ADVANCED MATERIALS LAB

## Abstract

Precipitated intermetallic phases strengthen aluminum aircraft alloys; these inclusions also establish localized electrochemical environments, significantly influencing the bulk corrosion behavior of such alloys. To gain insight on the effects of intermetallic phases on the bulk corrosion behavior, two established forms of electrochemical characterization techniques were used, polarization scans and impedance spectroscopy. This effort was undertaken to:

- Provide a statistical body of electrochemical data for aluminum alloys,
- Provide fundamental electrochemical parameters to aide in a continuum scale modeling effort,
- Validate the effect of solution chemistry on bulk corrosion behavior,
- Determine the influence of precipitated intermetallic phases on the bulk corrosion behavior,
- Decouple the metal-coating interface behavior from bulk corrosion behavior in continuing tests on coated aluminum.

## Introduction

The precipitated intermetallic phases in AA2024-T3 form localized galvanic couplings in the form of precipitate-matrix coupling, close-range precipitate-precipitate couplings in clusters, and long-range precipitate-precipitate couplings via conductive grain boundaries. Dealloyed particles result in a high $Cu^{2+}$ ion concentration in the bulk solution. Ions reduced on the surface of the metal, or on the surface of other precipitates, result in the production of $OH^-$ ions, and thus a local solution of high pH[1,2,3,4,5]. The specific interactions are as follows:

- Al-Cu and Al-Cu-Fe-Mn Precipitates
  - Form "blocky" particles cathodic to the matrix
  - Coupling of Cu-depleted matrix and Cu-rich particle establishes local potential, driving anodic trenching[2,3,4]
- Al-Cu-Mg (S-phase) Precipitates
  - Form spherical particles anodic to the matrix
  - most active, account for 60% of precipitated particles
  - Large cathode to anode ratio preferentially dealloys these particles
  - Reduction of Cu2+ ions drive surface pitting, grain boundary attack and cathodic trenching[2,3,4]

### Corrosion Behavior of Aluminum Alloys

**Pourbaix Diagram**

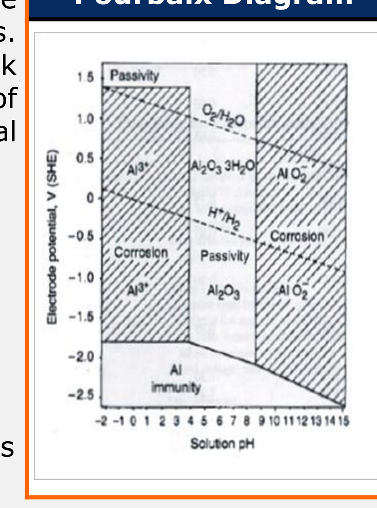

**IMC Schematic**

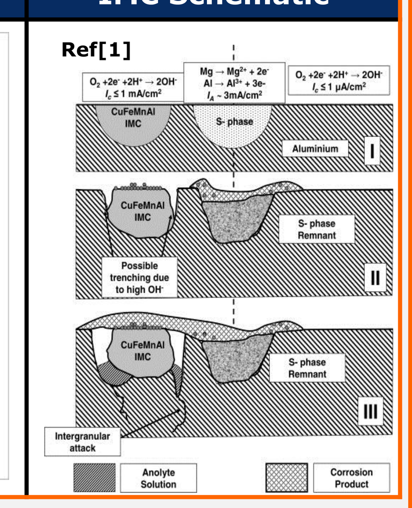


## Experimental

Polarization scans (DC) provided fundamental parameters such as open circuit potential, corrosion current density and Tafel slopes. Impedance spectroscopy (AC) provided parameters such as polarization resistance for extended durations. The test shown on the right were conducted in the setups shown below.

### Electrochemical Test Cells

**Flat Cell - DC**

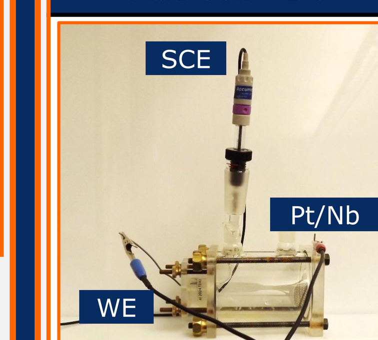


**Vertical Cell - AC**

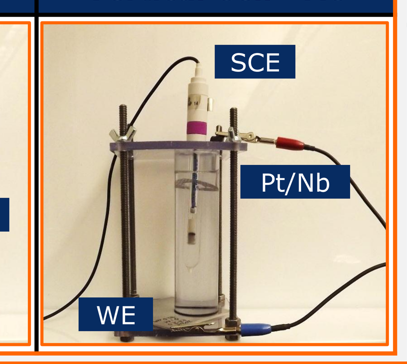


### Experimental Design Matrix

| Alloy | Electrochemical Test | Solution Chemistry | |
|---|---|---|---|
| Al 1100<br>• 99.0% Al min<br>• 0.95% Fe max<br>• 0.2% Cu max<br>• 0.05% Mn | Anodic Polarization Scan<br>• -20mV vs. OCP<br>• $10^{-3}$ A/cm2 turn-around | pH | 2.0, 4.0, 7.0, 10.0, 12.0 |
| | | [$Cl^-$] | 0.0M, 0.1M |
| | Cathodic Polarization Scan<br>• +20mV vs. OCP<br>• $10^{-3}$ A/cm2 turn-around | pH | 2.0, 4.0, 7.0, 10.0, 12.0 |
| | | [$Cl^-$] | 0.0M, 0.1M |
| | Electrochemical Impedance<br>• ±10mV vs. OCP,<br>• 0.01Hz ≤ f ≤ 1.0MHz | pH | 2.0, 4.0, 7.0, 10.0, 12.0 |
| | | [$Cl^-$] | 0.01M, 0.1M |
| Al 2024 – T3<br>• 4.60% Cu<br>• 1.50% Mg<br>• 0.65% Mn<br>• 0.16% Fe | Anodic Polarization Scan<br>• -20mV vs. OCP<br>• $10^{-3}$ A/cm2 turn-around | pH | 2.0, 4.0, 7.0, 10.0, 12.0 |
| | | [$Cl^-$] | 0.0M, 0.1M |
| | Cathodic Polarization Scan<br>• +20mV vs. OCP<br>• $10^{-3}$ A/cm2 turn-around | pH | 2.0, 4.0, 7.0, 10.0, 12.0 |
| | | [$Cl^-$] | 0.0M, 0.1M |
| | Electrochemical Impedance<br>• ±10mV vs. OCP,<br>• 0.01Hz ≤ f ≤ 1.0MHz | pH | 2.0, 4.0, 7.0, 10.0, 12.0 |
| | | [$Cl^-$] | 0.01M, 0.1M |

## Results

### Polarization Scans – DC Method

**AA1100 Summary**

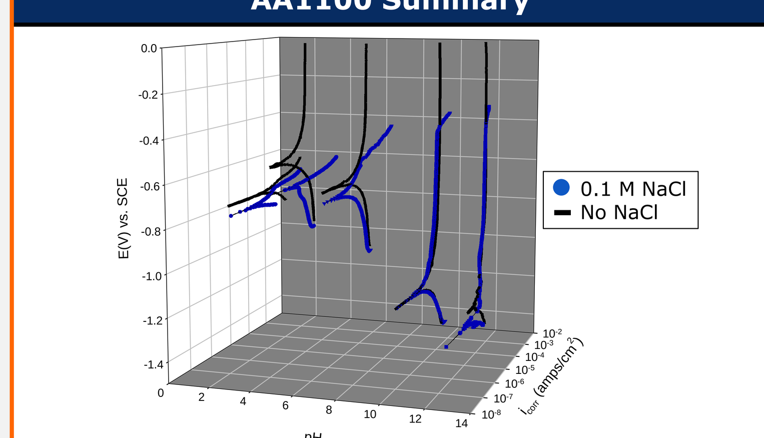


**AA2024-T3 Summary**

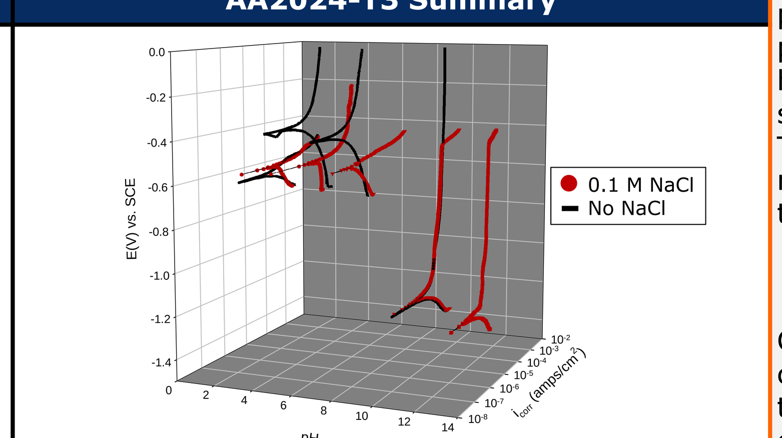


**Corrosion Potential**

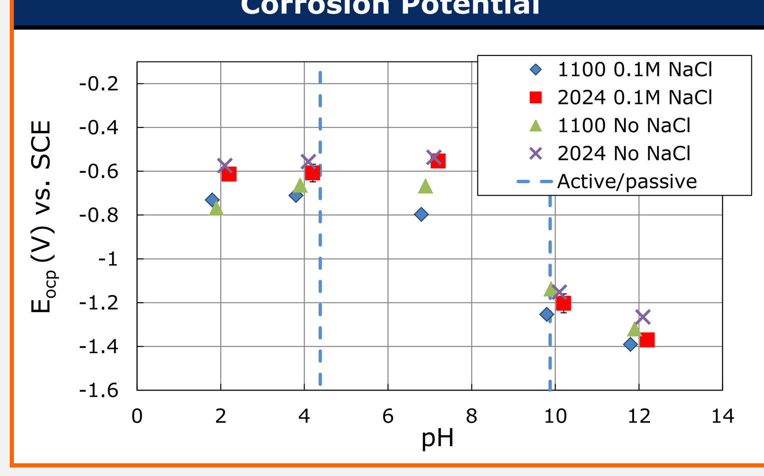


**Corrosion Current Density**

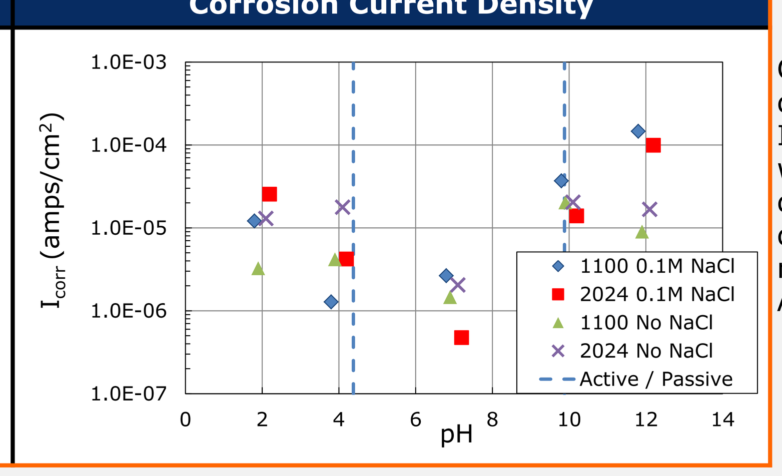


### Electrochemical Impedance – AC Method

**EIS Summary**

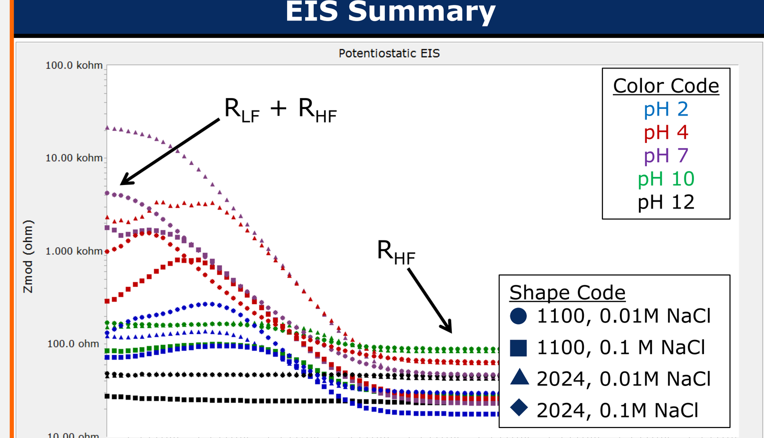


**AA1100 - $R_{LF}$ vs. Time**

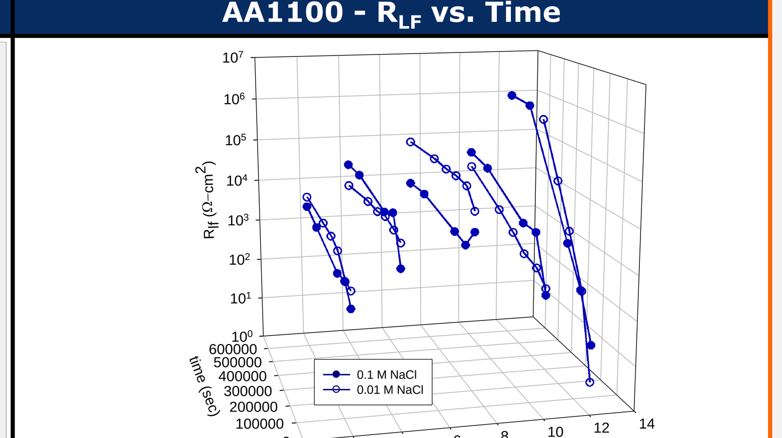

**AA2024T3 - $R_{LF}$ vs. Time**

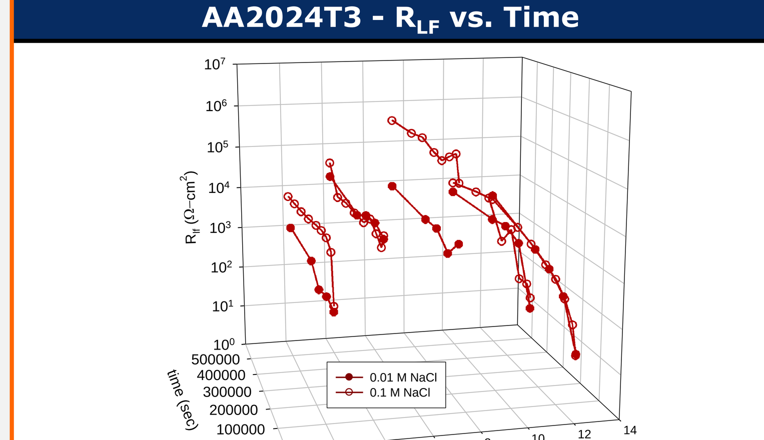

**Relationship of $R_{LF}$ and $I_{CORR}$**

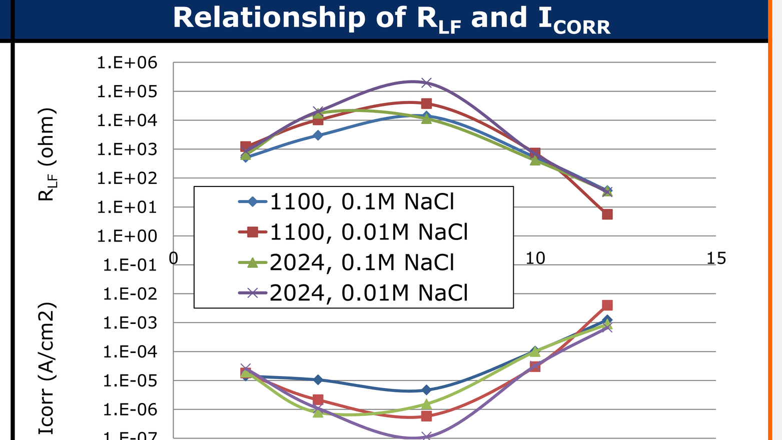


Experimental results, and the extracted parameters, can be seen in the series of plots at left, highlighting the polarization and impedance scans, the open circuit potentials, corrosion current densities, as well as the high and low frequency ($R_{HF}$, $R_{LF}$) resistance. Impedance spectroscopy was used to get $R_{LF}$ as a function of time. The corrosion current densities and low frequency resistances are related as follows, where βa and βc are the anodic and cathodic Tafel slopes.

$$R_{LF} = \frac{\beta_a \beta_c}{2.3 i_{corr}(\beta_a + \beta_c)}$$

Converting $R_{LF}$(time) to $I_{corr}$(time), the mass lost to corrosion can then be calculated as follows, where *a* is the atomic weight of the corroding species, *n* is equivalents per reaction and *F* is Faraday's constant.

$$m = \frac{I_{corr}(t)\, t\, a}{nF}$$

One can then predict a final solution concentration of dissolved ions after a specific time of exposure. Inductively coupled plasma mass spectroscopy (ICP-MS) was used to analyze the solution concentration of dissolved species following solution exposure for the duration of impedance scans, shown below. Measured results match closely with the predicted concentration of $Al^{3+}$.

### Something about calculated results

**Calculated Mass Lost to Dissolution of $Al^{3+}$**

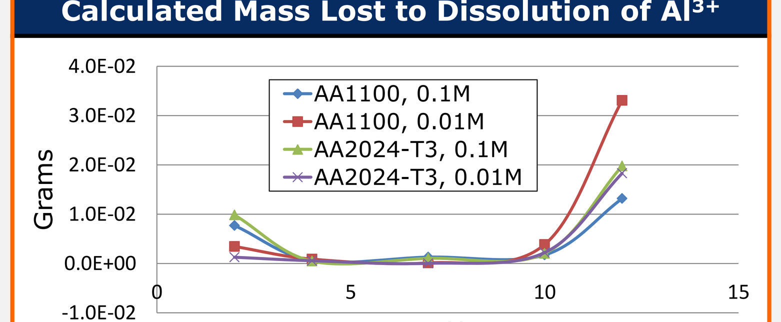


**Predicted Solution Concentration After 7 Days**

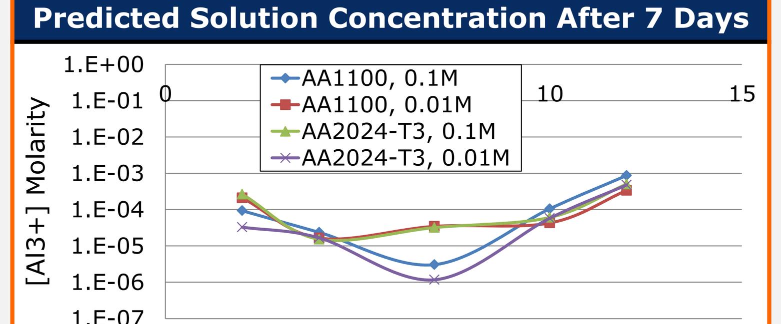


**ICP-MS AA2024T3, 0.1M NaCl**

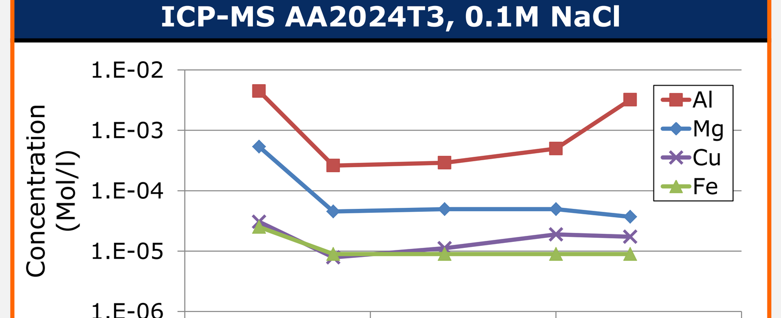


*The values at pH 2 have been inflated by an artificially induced corrosion potential.

## Discussion

### Precipitated Phases

**Backscattered SEM of AA2024-T3**

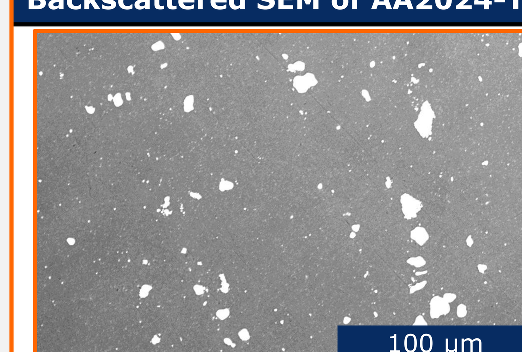


**Binary Image**

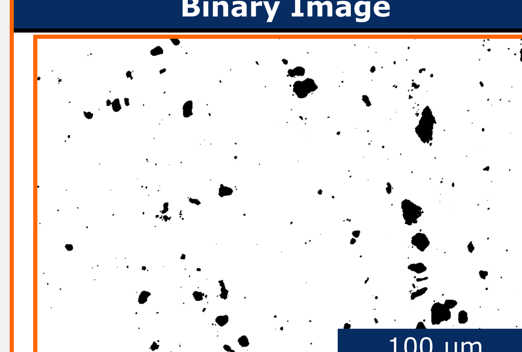


**Image Analysis Results**

| Slice | Count | Total Area | Average Size | %Area |
|---|---|---|---|---|
| 1.jpg | 470 | 1443.799 | 3.072 | 3.468 |
| 5.jpg | 3053 | 25959.487 | 8.503 | 2.482 |
| 11.jpg | 1145 | 1703.367 | 1.488 | 4.053 |
| 10.jpg | 1104 | 1082.629 | 0.981 | 2.572 |
| 9.jpg | 827 | 1411.777 | 1.707 | 3.349 |
| 8.jpg | 1577 | 1600.992 | 1.015 | 3.820 |

Surface particle analysis using ImageJ software suggests that approximately 3.5% of the exposed surface of AA2024-T3 is composed of precipitated phases.

**Particle Contributions**

The corrosion rates of select phases[1]

| Phase | OCP (mV) 0.1M NaCl | $I_{CORR}$ A/cm² @2024 OCP | $I_{CORR}$ A/cm² @own OCP |
|---|---|---|---|
| $Al_2CuMg$ | -830 (a) | 9.3E-3 | 1.1E-5 |
| $Al_7Cu_2Fe$ | -640 (a) | 3.8E-4 | 6.8E-5 |
| **AA2024-T3** | **-555** | **6.7E-6** | **6.7E-6** |
| $Al_2Cu$ | -484 (c) | 2.5E-6 | 3.5E-6 |

And contribution to total current[5]

| Steady State Dissolution | Al | Cu | Mg |
|---|---|---|---|
| Current Density (μA/cm²) | 2039 | 0.48 | 47.5 |
| Contribution (%) | Bal. | 0.023 | 2.3 |

### Particle Influenced Corrosion

**Corrosion Product Wedging - pH 7**


**Particle Induced Pitting – pH 4**

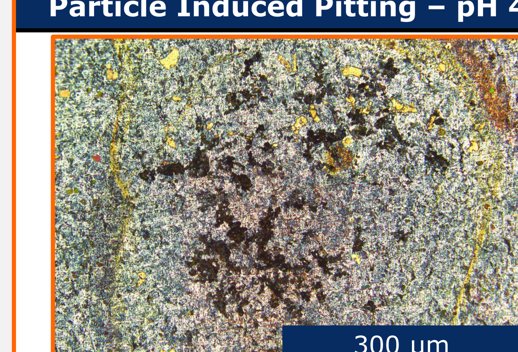


**Corrosion Product – pH 2**

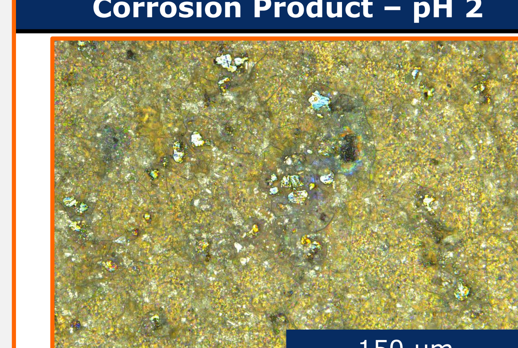


**Corrosion Product – pH 12**

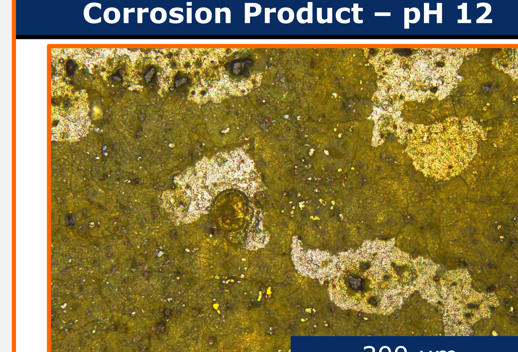


Corrosion of aluminum is dictated first by environmental exposure, and then influenced by microchemistry. Interactions of the matrix and precipitated phases in strengthened aluminum alloys result in localized methods of corrosion. Corrosion can lead to premature mechanical failure as a result of fatigue cracks initiating at pits, or cross-sectional reduction in area due to grain boundary etch-out. Coating failure can also be attributed to corrosion in the form of anodic undercutting, corrosion product wedging, cathodic delamination, a chemically induced loss of adhesion and osmotic effects.

This work set out to establish the effects of localized corrosion mechanisms on the bulk corrosion behavior. The exposed surface fraction of precipitated phases was determined to be approximately 3.5% using binary image analysis techniques on high-contrast, backscattered SEM images. Energy dispersive X-ray spectroscopy (EDS) confirmed the compositions of the "blocky" precipitates are of the Al-Cu and Al-Cu-Fe-Mn phases, and the spherical precipitates are of the Al-Cu-Mg, S-phase.

The specific dissolution rates of these particles[1] and their contribution to the overall current density[5] have been presented in literature and are in agreement with the values measured using ICP-MS. The observed mechanisms of corrosion influenced by the precipitated phases are also in agreement with those presented in literature[1,2,3,4,5].

The fundamental parameters extracted from these data can be used in the equations governing the corrosion behavior of aluminum. With a thorough understanding of this behavior, the corrosion of bare and coated aluminum alloys can be modeled in a range of environments.

### Corrosion Modeling

**$E_{CORR}$ and $I_{CORR}$ as Functions of pH**

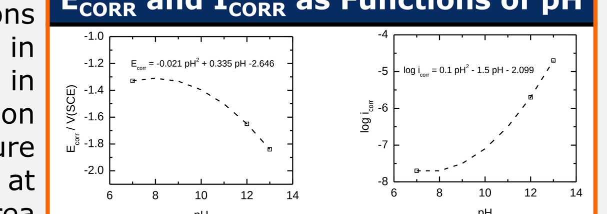


| Parameter | pH 7 | pH 12 | pH 13 |
|---|---|---|---|
| $E_{CORR}$ (V) | -1.33 | -1.65 | -1.84 |
| $I_{CORR}$ (A/cm²) | 2.0E-8 | 2.0E-6 | 2.0E-5 |
| $\beta_{Al}$(mV.dec⁻¹) | 733 | 93 | 78 |
| $\beta_{H2}$(mV.dec⁻¹) | 43 | 52 | 55 |

**Simulated Polarization Curves**

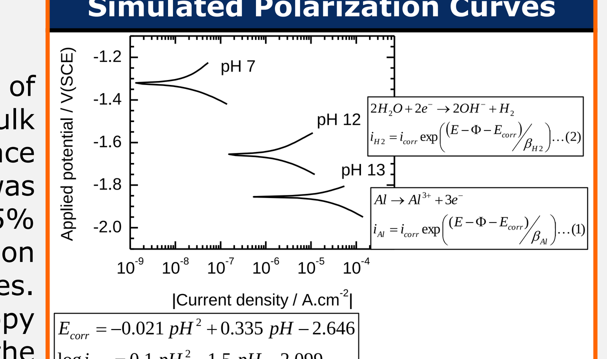


**Coating and Electrolyte pH**

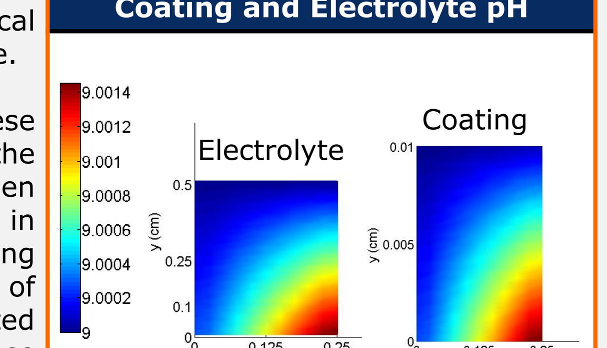


**Modeling Commentary**

1. Fundamental parameters derived from experimental data build expressions for corrosion behavior as a function of pH
2. Polarization scans can be simulated from expressions
3. Localized corrosion can be modeled in a variety of systems

## Conclusions

- This work has provided a statistical body of electrochemical data to the open literature for aluminum alloys 1100 and 2024-T3
- The fundamental parameters determined by this work will aide in the modeling of corrosion on a continuum scale
- The effect of solution chemistry was verified on the bulk corrosion behavior of aluminum, and corrosion rates for a comprehensive set of solutions was provided
- The localized corrosion mechanisms influenced by the presence of precipitated intermetallic phases was shown to influence the bulk corrosion behavior, and can be measured with a globalized test
- This work will aide in a modeling effort to decouple the metal-coating interface behavior from bulk corrosion behavior in continuing tests on coated aluminum alloys

BOEING

## Acknowledgements

- This project has been generously supported by the Boeing Company
- A special thanks to Erik Sapper and the Boeing Research and Technology department for their enthusiastic encouragement
- Our gratitude to Anthony Brown of the Boise State department of Geosciences for providing ICP-MS analysis

## References

[1] Boag, A., R.J. Taylor, T.H. Muster, N. Goodman, D. McCulloch, C. Ryan, B. Rout, D. Jamieson, and A.E. Hughes. "Stable Pit Formation on AA2024-T3 in a NaCl Environment." *Corrosion Science* 50 (2009): 30-103. Print.
[2] Glenn, A.M., T.H. Muster, C. Luo, X. Zhou, G.E. Thompson, A. Boag, and A.E. Hughes. "Corrosion of AA2024-T3 Part III: Propagation." *Corrosion Science* 53.1 (2011): 40-50.
[3] Ilevbare, G. O., O. Schneider, R. G. Kelly, and J. R. Scully. "In Situ Confocal Laser Scanning Microscopy of AA 2024-T3 Corrosion Metrology." *Journal of The Electrochemical Society* 151.8 (2004): B453-472.
[4] King, Peter C., Ivan S. Cole, Penny A. Corrigan, Anthony E. Hughes, and Tim H. Muster. "FIB/SEM Study of AA2024 Corrosion under a Seawater Drop." *Corrosion Science* 53 (2011): 1086-096.
[5] Mokaddem, M., P. Volovitch, F. Rechou, R. Oltra, and K. Ogle. "The Anodic and Cathodic Dissolution of Al and Al–Cu–Mg Alloy." *Electrochimica Acta* 55.11 (2010): 3779-786.

CAES